JOURNAL OF GEOPHYSICAL RESEARCH, VOL. 105, NO, D8, PAGES 9887–9901, APRIL 27, 2000

Measurement of atmospheric optical parameters on U.S. Atlantic coast sites, ships, and Bermuda during TARFOX

A.Smirnov[1,2], B.N.Holben[1], O.Dubovik[1,2], N.T.O'Neill[1,4], L.A.Remer[3], T.F.Eck[1,5], I.Slutsker[1,2], and D.Savoie[6]

Abstract. The Aerosol Robotic Network (AERONET) of automatic Sun/sky radiometers collected data on U.S. Atlantic coast sites, ships, and Bermuda in 1996 during the Tropospheric Aerosol Radiative Forcing Observational Experiment (TARFOX). Spatial and temporal analysis of Sun photometry data was supported by synoptic analysis of air mass evolution. The spatial distribution of aerosol optical depth is presented. In several cases the aerosol size distributions deduced from sky almucantar measurements and solar disk attenuation measurements at the various coastal sites yielded similar results within the same air masses. Ship-based measurements in the Atlantic Ocean showed significant maritime aerosol optical property variations which for the most part could be attributed to the influence of continental sources and Saharan dust events. The Bermuda data (optical depths and Angstrom parameter values) illustrated changes in atmospheric optical properties for various air masses and trajectories. Almost no correlation was observed between aerosol optical depth and water vapor content when the data from all stations and ship measurements were considered together. In the case of individual stations or ship transects, different degrees of correlation could be observed. In continental conditions on the east coast, optical depth and water vapor are well correlated, while in a maritime environment, optical depth can be relatively small despite high water vapor contents.

1. Introduction

The Tropospheric Aerosol Radiative Forcing Observational Experiment (TARFOX) was conducted in July 1996. The principal design objective of TARFOX was to achieve a short-term U.S. eastern seaboard-wide understanding of the atmospheric optical parameters which significantly influence direct radiative forcing *[Russell et al.,* 19991. The temporal and spatial variability of the vertically integrated optical parameters acquired by Sun photometers and sky-scanning radiometers provide a key contribution to this understanding.

Spatial, temporal, and vertical structures of atmospheric aerosol optical parameters along with the aerosol-type information is required globally for an assessment of the radiative forcing [*Kaufman et al.,* 19971.

The Aerosol Robotic Network (AERONET) is a worldwide network of Sun/sky radiometers which perform a dual role of spectral Sun photometry as well as spectral sky-scanning radiometry [*Holben et al.*, 19981. Such measurements yield basically two types of vertically integrated optical information: aerosol optical depth and the product of aerosol optical depth with the scattering phase function. The magnitude of the former parameter yields vertically integrated indicators of aerosol number density or concentration, while its spectral dependency contains (mostly submicron) aerosol-sizing information. The magnitude of the latter parameter again contains information on integrated aerosol concentration, while its angular dependency is an indicator of (both submicron and supermicron) aerosol particle size.

The spatial density of AERONET stations is the result of many considerations, including the heritage of existing meteorological infrastructures. Aerosol optical properties are strongly dependent on the evolution of synoptic air masses and associated source regions and to a certain extent can be uniquely characterized by the air mass type and source [*Smirnov et al.*, 1995a]. An air mass, in the classical sense, is a large homogeneous volume of air characterized by a certain vertical profile of temperature and humidity. Atmospheric aerosol optical properties and concentrations are expected to be reasonably uniform within an air mass. The goal of the current consideration is to study the effect of various aerosol source regions on the optical properties of a cloudless atmosphere.

The overall goal of the present paper is to investigate, within the TARFOX context, the effect of various types of air masses on the optical properties of the U.S. eastern seaboard atmosphere

[1] NASA Goddard Space Flight Center, Biospheric Sciences Branch, Greenbelt, Maryland.
[2] Also at Science Systems and Applications, Inc., Lanham, Maryland.
[3] NASA Goddard Space Flight Center, Climate and Radiation Branch, Greenbelt, Maryland.
[4] Also at Centre d'Applications et de Recherches en Teledection, Universite de Sherbrooke, Sherbrooke, Quebec, Canada.
[5] Also at Raytheon ITSS Corporation, Lanham, Maryland.
[6] Division of Marine and Atmospheric Chemistry, University of Miami, Miami, Florida.

Paper number 1999JD901067.
0148-0227/00/1999JD901067$09.00

under conditions of low cloud fraction. The methodology revolves around the temporal and spatial analysis of Sun photometry data obtained at various land-based and shipboard sites in conjunction with information on air mass origin and evolution. Our principle objective is to better characterize the multisite variability of aerosol optical depth within the same air mass.

2. Instrumentation, Data Collection, and Cloud-Screening Procedure

The AERONET network of automatic Sun/sky radiometers collected data on **U.S.** mid-Atlantic east coast sites in July 1996 during TARFOX. The instrument deployed in the network is the automatic Sun- and sky-scanning radiometer CIMEL CE-318. This instrument measures the direct Sun radiance in eight spectral channels within the 340 to 1020 nm spectral range and sky radiances in a subset of four spectral channels *[Holbenet al.,* 19981. The bandwidths (full widths at half maximum) of the interference filters employed in these radiometers vary from 2 to 10 nm. The ratio of transmittance in the wings to the maximum transmittance of the filters is less than 10^{-4}. Although the CIMEL instruments are not temperature stabilized, their temperature is routinely monitored. Temperature correction is systematically applied to the 1020 nm channel voltages as recommended by the manufacturer and verified and quantified by laboratory temperature testing.

The direct Sun measurements are acquired in approximately 10 s across the eight spectral bands. A sequence of three such eight band measurements are taken 30 s apart to yield one triplet observation per wavelength [*Holben et al.*, 19981. Seven of the eight bands are used to acquire aerosol optical depth data. The eighth band at 940 nm is used to estimate total precipitable water content. The details of the water vapor content extraction procedure and the types of errors involved can be found in the work of *Halthore et al.* [1997]. *Eck et al.* [1999] presented careful assessments of total uncertainty in computed τ_a for field instruments. Calibration and computation errors overall yielded a total uncertainty of –0.01-0.02, which is spectrally dependent with the higher errors in the **UV** spectral range. *Schmid et al.* [1999] performed the comparison of five solar-tracking radiometers for measuring total optical depth. Discrepancies between aerosol optical depths measured by CIMEL Sun photometer and other instruments were not higher than 0.015 (rms).

The accuracy of the aerosol particle size distributions retrieved from Sun and sky radiances measured with CIMEL radiometers has been studied in detail by Dubovik et al. [1999b]. The retrieval residuals resulting from random errors, possible instrumental offsets, and known uncertainties in the atmospheric radiation model have been analyzed. Sky radiances and aerosol optical depths obtained by reinserting the retrieved size distributions back into the radiative transfer calculations resulted in differences of less than 5% compared to measured values. We also estimated errors in dV/d ln R based on the methodology described by Dubovik et al. [1999b]. Retrieval errors should not exceed 15-20% for particle sizes within 0.1-7 μm range. The errors in the tails of the particle size distributions (for the very small and very large particles) may be as large as 35-100%; however, no significant shifts in the positions of mode radii or changes in the shape of size distributions are expected.

An automatized and computerized cloud-screening algorithm *[Smirnov et al.*, Cloud screening and quality control algorithms for the AERONET database, submitted to *Remote Sensing of Environment,* 19991 was applied to the direct Sun measurements. Two major criteria were employed in the cloud-screening procedure. First, we retained stable triplets in order to eliminate high-frequency changes. Since the optical variation of clouds is typically greater than that of aerosols, the triplet variation can be **used** in many cases to screen clouds. Assuming that optical depth variability within a triplet should not be higher than the accuracy of our measurements (±0.01), we, in the first instance, accept all $\tau_i(\lambda)$ when $(\tau_{max} - \tau_{min}) \leq 0.02$. This constraint simply means that atmospheric optical properties should be relatively stable within 60-70 s. Thus we define $\tau_i(\lambda)^{good}$ for each triplet observation. Secondly, rapid temporal optical depth variations ("spikes") between selected triplets are eliminated by applying a root-mean-square second-derivative threshold. From a physical point of view, $\tau_a(\lambda)$ cannot undergo large rapid changes (except in narrow plumes) and qualified smoothness in time and space is expected. In other words, the smoothness criterion is based on the idea of limiting sudden increases and decreases of optical depth. These conditions imposed on aerosol optical depth diurnal variability are not excessive and do not significantly bias daily averages [*Smirnov et al.*, Cloud screening and quality control algorithms for the AERONET database, submitted to *Remote Sensing of Environment,* 1999].

In our final cloud-screening data check the Angstrom parameter, as estimated using a least square method, is analyzed. Even if the aerosol optical depth spectrum is not well represented by the power law $(\lambda^{-\alpha})$ the Angstrom parameter α can still be considered as a mean indicator of its spectral behavior. One of the indicators of cloud contamination is a small Angstrom parameter combined with a large optical depth. Accordingly, the spectral dependence of aerosol optical depth can be used to further screen the data in the case of continental nondust aerosols, Approximately 50-60% of the original data remained after the application of the complete screening procedure, including all above mentioned checks.

3. Atmospheric Optical Properties on U.S. Mid-Atlantic East Coast Sites

Aerosol optical properties were derived from direct Sun and sky radiation measurements performed at the operational sites of the AERONET network, namely, Sandy Hook, New Jersey (40" 25' N, 73° 59' W, elevation 2 m), Goddard Space Flight Center (GSFC), Greenbelt, Maryland (39° 01' N, 76° 52' W, elevation 50 m), Wallops Island, Virginia (37" 56' N, 75° 28' W, elevation 10 m), Hog Island, Virginia (37" 25' N, 75° 42' **W,** elevation 50 m), Cheritan, Virginia (37° 16' N, 75° 25' W, elevation **2** m), and Hampton Roads, Virginia (37" 46' N, 76" 26' W, elevation 10 m). The instrument at Hog Island was relocated to Cheritan in the middle of the month. Figure 1 shows the locations.

The spectral aerosol optical depth measurements from the east coast sites were analyzed as a function of air mass source region. The objective is to understand the variability of aerosol optical depth within a given air mass as it passes over each site. Air mass back trajectory analyses for various pressure levels (1000, 925, 850, and 700 mbar) permit a better understanding of atmospheric optical property variations associated with the modification of air masses due to the variability of trajectories and local terrestrial

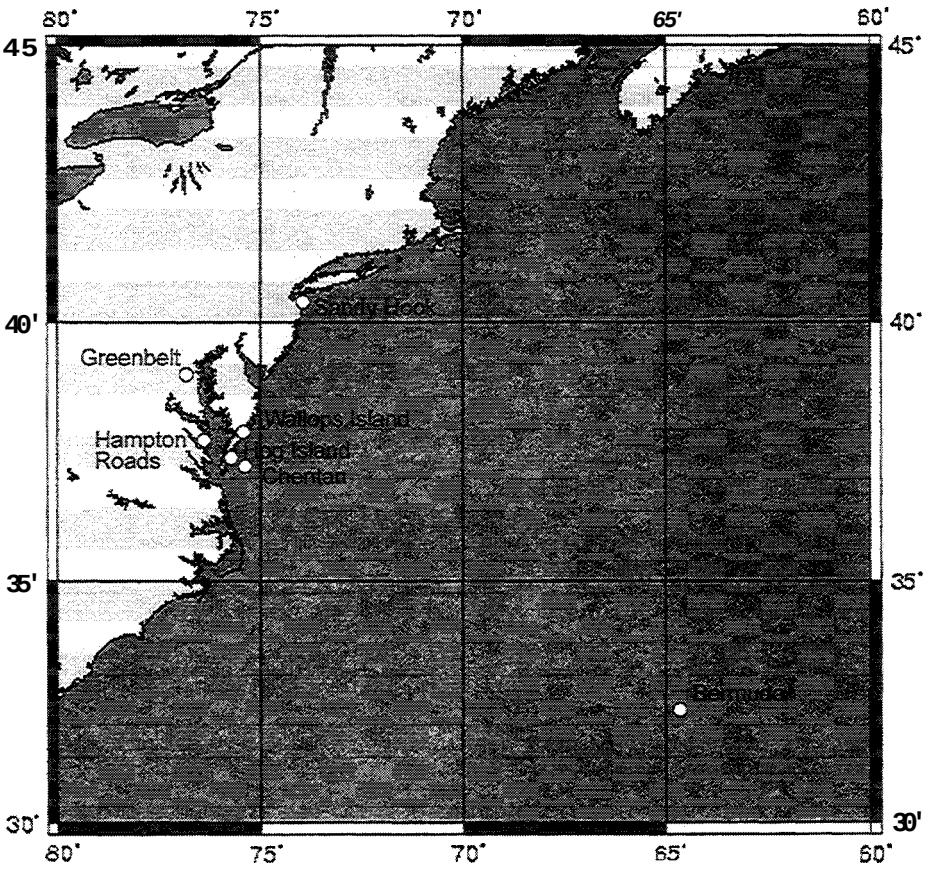

Figure 1. Map of the seven Aerosol Robotic Network sites used in the study.

aerosol sources. Plate 1 is indicative of the variety of synoptic situations that occurred during the month of July 1996. Back trajectories were simulated at the Atmospheric Environment Service of Environment Canada using the same algorithm as in the work of *Leaitch et al.* [1996].

Daily averages of τ_a(500 nm) for the east coast sites are shown in Figure 2. A large variability both temporally and spatially is evident from this graph. Generally, we are able to distinguish aerosol optical properties for air masses from the northern sector and southwestern sector. Continental polar air from the North (CPN) (Canadian Arctic or Hudson Bay) has brought relatively cool and clean air (low τ_a) and low total precipitable water. Maritime tropical airflow from the southeastern states and the Gulf of Mexico as well as from the western sector brought humid polluted air, causing optical depth to increase by a factor of **2,** at least, compared to the clean CPN conditions.

It is evident that southwestern airflow brings moist and turbid air to all sites considered. To clarify this point, we present, in Table 1, mean aerosol optical depth at 500 nm and water vapor content for three air mass source regions at pressure level 1000 mbar. Standard deviations are presented in parentheses. It is notable that statistical characteristics are quite similar between the averaged data at the GSFC site and the averaged data for all sites (Table 1).

The scattergram in Figure 3 demonstrates how daily averages of aerosol optical depth correlate with the total precipitable water amount (or water vapor content in centimeters, extracted according to *Halthore et al.* [1997]). For the whole data set an exponential fit explained 76% of the variance:

$$\tau_a\,(500\,\text{nm}) = 0.038\exp(0.732\text{WVC}),$$

where WVC is the water vapor content (precipitable water) in the total atmospheric column (in centimeters). The high correlation exhibited in the relationship can be explained by the previously mentioned influence of different trajectories and by the growth of hygroscopic particles at increasing relative humidities *[Kotchenruther et al.,* 19991.

Atmospheric optical parameters associated with polar air from the north were spatially homogeneous on July **4** for a transect stretching from Sandy Hook, New Jersey, to Hampton Roads, Virginia. Figures 4a and 4b show the spectral dependence of aerosol optical depth and volume size distributions retrieved from solar almucantar sky measurements and solar disk attenuation measurements using the algorithm developed by *Dubovik et al.* [1999a].

Air amving from the Gulf of Mexico and southeastern states on July 6 and **7** induced significant changes relative to the situation on July **4** and 5. The aerosol optical depth increased by a factor of **4,** while its spectral slope increased (Figure 5a). The similarity of optical properties across all the sites is evident in Figure 5a. Volume size distributions are consistent and are in qualitative agreement with the aerosol optical depth data;

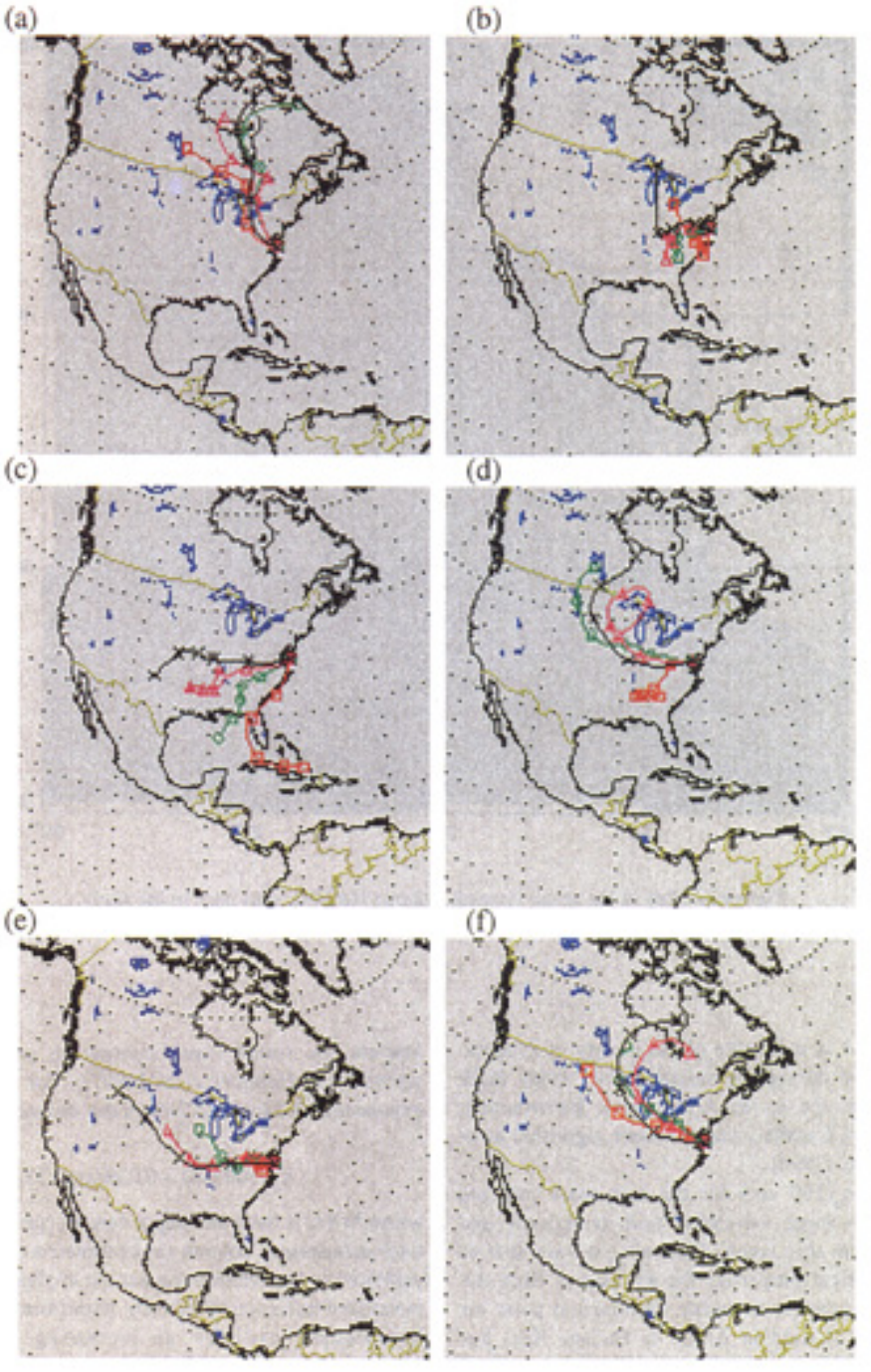

Plate 1. Selected set of 5-day back trajectories showing sources for air at 1000 mbar (red), **925** mbar (green), 850 mbar (purple), and **700** mbar (black) for the Wallops Island site on July **4,** 1800 UT (a), July **7,** 1800 UT (b), July 8, 1800 UT (c), July **26,** 1800 UT (e), July **27,** 1800 UT (f), and for the Goddard Space Flight Center site on July **16,** 1800 UT (d).

between Figures 4b and 5b we note that the accumulation mode **(0.3-0.6** μm) increase is significantly greater than the coarse particle mode (0.7-15 μm) increase.

Optical properties and volume size distributions for a variety of synoptic situations are presented in Figures 6a and 6b. The northern, southern, western, and northwestern flows presented in Plate 1 induced the variety of optical conditions, which are evident in these two figures. Synchronous changes in τ_a or volume size distributions could not be observed simultaneously at each location because of the presence of clouds over alternating portions of the Sun photometer network. Nevertheless, the dynamics of $\tau_a(h)$ and $dV/d\ln R$ can still be observed. We would even argue that for more humid air with higher amounts of precipitable water and higher τ_a that the fine

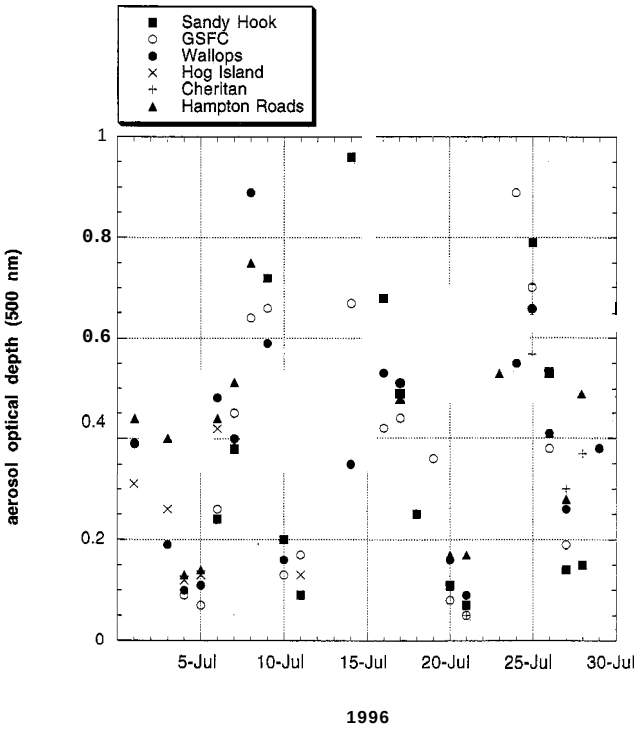

Figure 2. Daily averages of aerosol optical depth at 500 nm for the east coast sites.

fraction maximum shifted slightly toward bigger radii (Figure 6b), although not for every case. The position of the fine fraction maximum is consistent with the model of ***Remer and Kaufman*** [1998], but our coarse mode yielded values smaller than those predicted by the latter model. Agreement for the coarse mode is better with the modified model presented by ***Remer et al.*** [19991.

4. Bermuda Measurements

A CIMEL Sun photometer was located at the Bermuda Biological Station (32°22' N, 64°41' W, elevation 10 m). Daily averages of τ_a(500 nm) and its standard deviation are shown in Figure 7a. For days with no Saharan dust the mean τ_a(500 nm) varies between *0.05* and 0.33, while ranging from 0.28 to 0.45 during the Saharan dust events on July 7, 10, 11, 12, and 24. The Angstrom parameter α for non-Saharan dust cases is within the 0.4-1.9 range, while decreasing to values in the range 0.2-0.5 in dusty conditions (Figure 7b). It should be noted that in the afternoon of July 24, α was about 0.8-0.9, despite the presence of dust. Size distribution retrievals indicated that along with the coarse fraction typical of dust a significant number of small particles greatly contributed to the aerosol size spectra on this day.

During the month of July 1996 we had an opportunity to observe three different optical conditions associated with various aerosol sources which we defined in terms of generalized source trajectories: Saharan dust, pure Atlantic air, and air from North America. A selected set of five-day back trajectories at 1000, 925, 850, and 700 mbar is presented in Plate 2. There is not enough evidence to clearly show the source of Saharan dust given only the 120 hours (five days) back trajectories. It is well known, however, that the Saharan aerosol layer is located above 3 km (above our 700 mbar pressure level) [*Prospero and Carlson*, 19721. As well, it would have been better to analyze the back trajectories of such long-distance oceanic air parcels for a longer period of time, say, 7 or even 10 days back.

Changes in atmospheric optical properties for various air masses are illustrated in Figure **8.** Dusty conditions predominated on July 10, while pure maritime conditions prevailed on July 14. On July 30 the air was greatly influenced by North American continental sources. Figure 8a shows aerosol optical depths and their spectral dependencies. As would be expected, continental air is more turbid (greater aerosol optical depth at 500 nm wavelength) than maritime air. Also, it can be noted that the spectral behavior of $\tau_a(\lambda)$ is more selective in continental air masses (higher Angstrom parameter value corresponding to generally larger extinction contributions from smaller particles). The corresponding bimodal aerosol volume size distributions, retrieved from the sky radiance and direct solar extinction measurements ***[Dubovik et al.,*** 1999a] can be observed in Figure 8b. Columnar size distributions indicate **two** modes (fine and coarse). The position of the fine mode maximum for all three distributions, as well as of the coarse mode for the dusty conditions, is consistent (within f0.05 μm) with the reported results ***[Porter and Clarke,*** 1997; ***Quinn et al.,*** 1996; ***Gerber,*** 1991; ***Shettle and Fenn,*** 19791.

5. Atlantic Ocean Measurements

Measurements in the Atlantic Ocean between New **York** City and Bermuda were carried out onboard two cruise ships. This series of measurements was the first time the CIMEL Sun

Table 1. Mean Aerosol Optical Depth and Water Vapor Content for Three Air Mass Source Regions

Air Mass Source Region at 1000 mbar (Days Included in Category)	GSFC Site		All Sites	
	Mean τ_a(500 nm) and s.d.	Mean WVC (cm) and s.d.	Mean τ_a(500 nm) and s.d.	Mean WVC (cm) and s.d.
Northern airflow (July 4, 5, 11, 20, 21)	0.09 (0.04)	1.38 (0.30)	0.11 (0.04)	1.61 (0.25)
Southern airflow (July 8, 15, 16)	0.53 (0.16)	3.73 (0.91)	0.65 (0.17)	3.69 (0.66)
Western airflow (July 1, 2, 3, 9, 10, 17, 18, 26, 27)	0.36 (0.19)	2.84 (0.78)	0.38 (0.17)	2.89 (0.55)

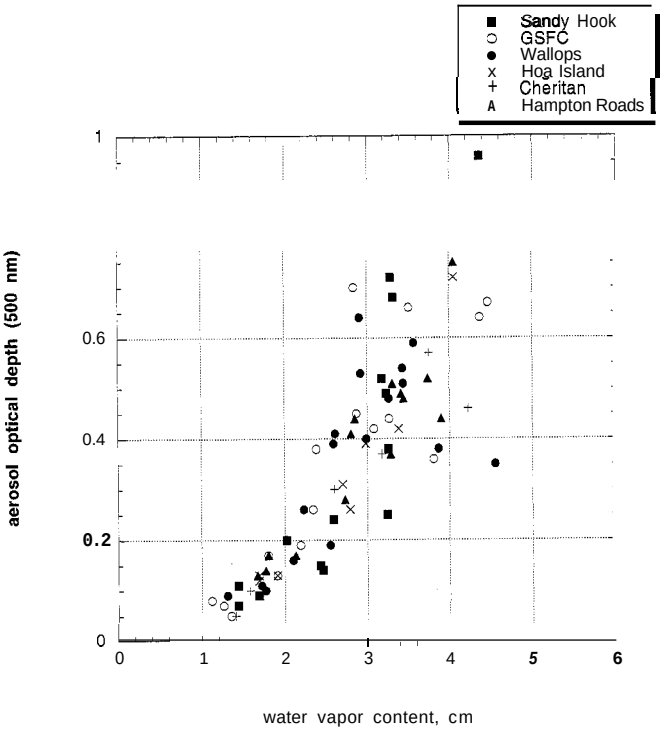

Figure 3. Scattergram of daily averages of aerosol optical depth at 500 nm versus water vapor content in centimeters of precipitable water.

photometer was deployed at sea by our project team. The weather conditions were not favorable for Sun measurements (significant high-altitude cirrus). However, in at least two cases, where cloud cover was scattered, we were able to monitor aerosol optical depth variability throughout the day. These observations, supported by the operator's remarks, provided some interesting data for our analysis of the temporal and spatial variability of aerosol optical parameters above the ocean. Simultaneous sky radiance measurements were problematic because of the vibration of the ship and wave-induced motion, and accordingly, such inversions for aerosol microstructure were performed only occasionally. Almucantars in all spectral channels were not sufficiently symmetrical to permit inversions for aerosol microstructure due in part to the 4-min scan time for an almucantar measurement sequence. To achieve an acceptable consistency, we employed only sky radiances at a wavelength of 1020 nm, thus limiting the scan time to 1 min. The almucantar symmetry of the radiances in this channel was judged to be satisfactory on a number of occasions.

Table 2 gives the details of the cruises, dates, and latitude-longitudes. The instantaneous position of the ships was obtained from an onboard Global Positioning System.

The diurnal variability of aerosol optical depth on July 8 is presented in Figure 9a. Optical depth decreased gradually while the ship was moving in a direction away from the continent and remained stable for the rest of the day. The $\tau_a(\lambda)$ spectral dependence remained stable ($\alpha \sim 1.8$) despite changes in τ_a (500 nm) by a factor of 2. The high morning turbidity is associated with high concentrations of small urban/industrial continental

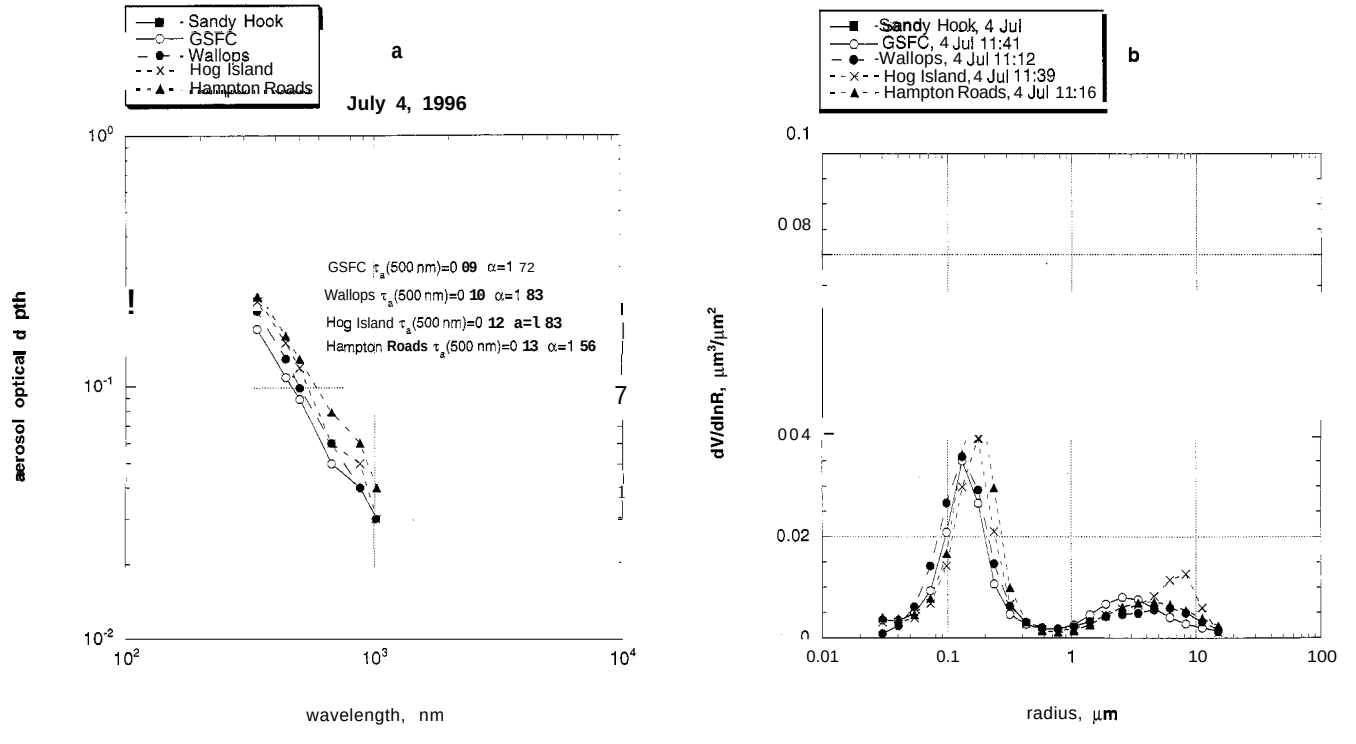

Figure 4. Aerosol optical depth spectra for the east coast sites on July 4 (a) and retrieved aerosol volume size distributions (b).

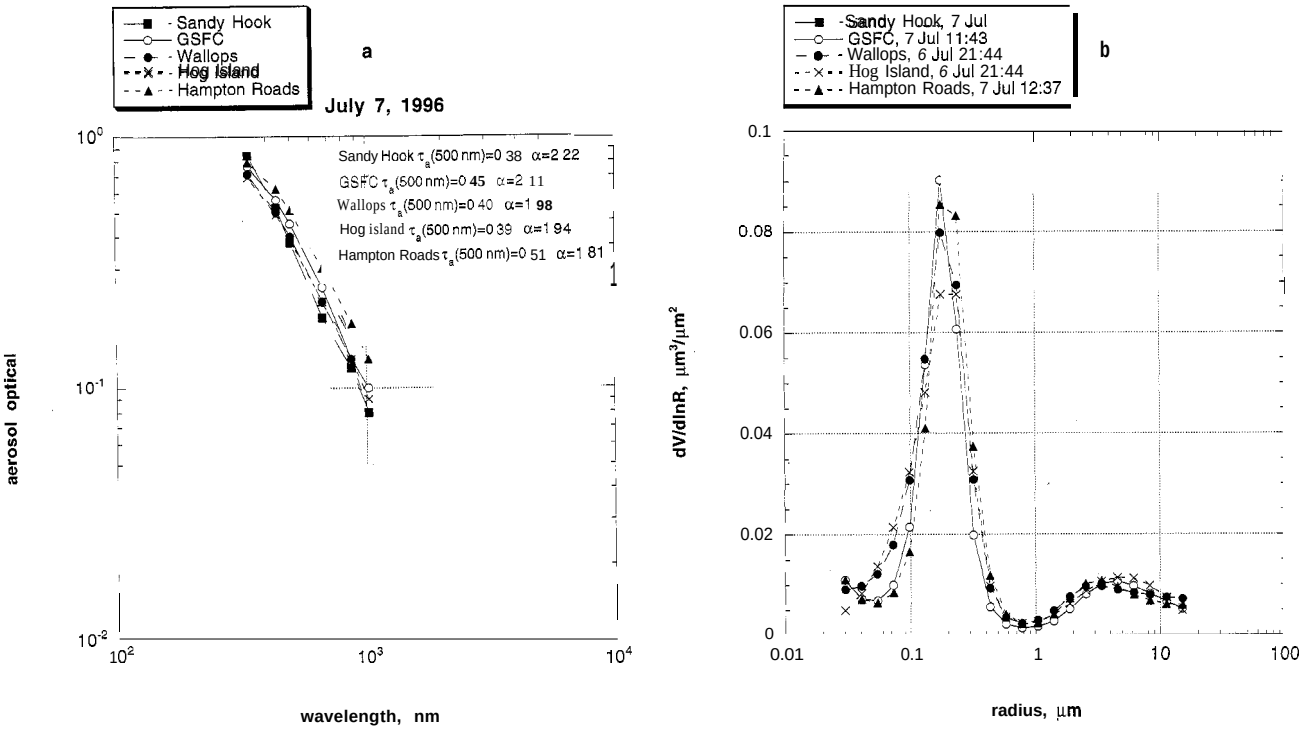

Figure 5. Aerosol optical depth spectra for the east coast sites on July 7 (a) and retrieved aerosol volume size distributions (b).

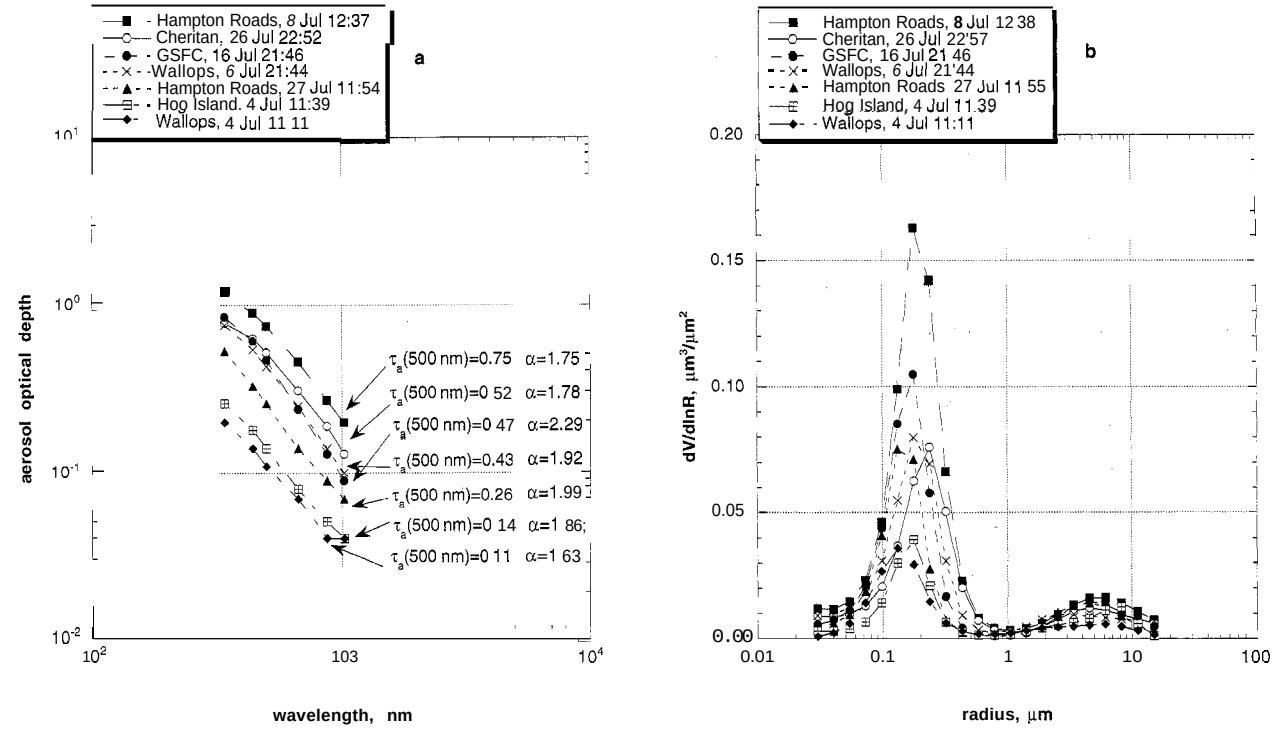

Figure 6. Aerosol optical depth spectra (a) and retrieved aerosol volume size distributions (b) for a variety of synoptical situations on the east coast sites.

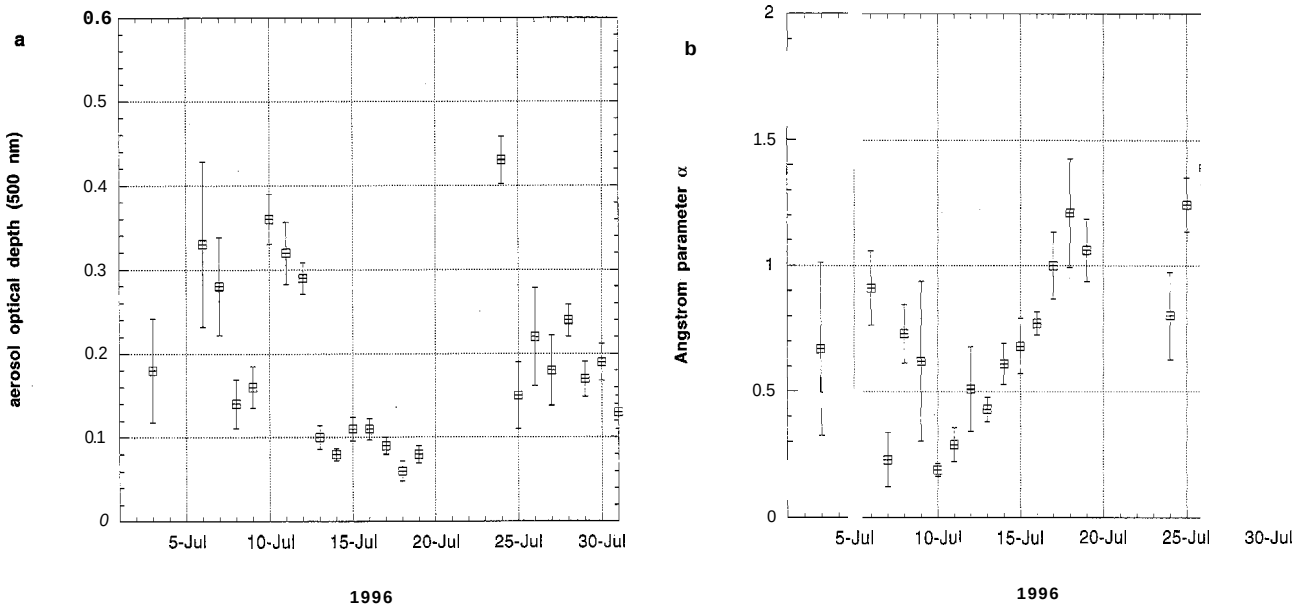

Figure 7. Daily averages of aerosol optical depth at 500 nm (a) and Ängström parameter (b) for the island of Bermuda. The bars indicate plus or minus one standard deviation.

aerosols (a −1.8). Even in the afternoon, the aerosol optical depth was larger and more spectrally dependent than reported in the literature for remote Atlantic conditions [*Hoppel et al.,* 1990; ***Reddy et al.,*** 1990; *Smirnov et al.,* 1995b]. The back trajectory analysis confirmed that air originating above the continent was responsible for the relatively high aerosol loading in the measurement area (Plates 3a and 3b).

On July 27 the optical conditions underwent significant changes (Figure 9b). Nevertheless, diurnal variations of the Ängström parameter were rather small. Turbid optical conditions in the morning (τ_a (500 nm) −0.4, α~1.6) evolved into an unusually hazy event with τ_a (500 nm) −0.7 and a−1.7. Ship-based observers did not see any clouds, and the solar disk seemed to be unobscured. One cannot exclude the presence of subvisual clouds, but their impact on total optical depth would be rather small [*Sassen et al.*, 19891. Around 1700 UT the optical depth and the Angstrom coefficient returned to values similar to the morning conditions and stayed stable for several hours. About 1930 UT the values of τ_a (500 nm) decreased again by a factor of 2 but ***a*** remained unchanged (−1.7). Optical parameters remained stable during late afternoon hours. Back trajectories indicated that continental air greatly influenced optical properties in this area of the Atlantic Ocean (Plates 3d-3f). Unlike the July 8 back trajectories at the 1000 mbar level, however, the July 27 source positions changed during the day from southern to western and northwestern in the late afternoon. Western sector trajectories at the 925 and 850 mbar level dominated throughout most of the day while gradually shifting to the northern sector by late afternoon. Clean air from the north changed optical conditions, and the aerosol optical depth decreased.

Figure 9c shows aerosol optical depth diurnal variations in the presence of Saharan dust on July 12. These measurements were carried out near Bermuda and, not surprisingly, show that on average τ_a (500 nm) and ***a*** were similar to the land values obtained for July 10-12 on Bermuda (Figure 7b). One hour of measurements acquired on the afternoon of July 25 is presented in Figure 9d. One can observe a slight increase in optical depth, while the Angstrom parameter remains almost unchanged (a−1.25). According to ***Reddy et al.*** [1990] such optical

Table 2. Cruises Summary (Ship Positions)

Date	UT	Lat N	Long W
08/07/96	1139	37.39	70.06
08/07/96	2009	35.35	67.81
09/07/96	1015	32.47	64.58
12/07/96	1603	32.63	64.72
12/07/96	2140	33.64	65.75
18/07/96	1814	32.37	64.70
18/07/96	2013	32.78	64.87
20/07/96	1832	37.38	69.96
20/07/96	2307	38.46	71.32
21/07/96	1032	37.51	70.21
21/07/96	1414	36.63	69.18
25/07/96	1959	32.70	64.72
25/07/96	2055	32.92	64.95
26/07/96	1304	36.74	68.48
26/07/96	2043	38.17	70.89
27/07/96	1222	35.85	68.33
27/07/96	2238	38.24	71.09

Read 08/07/96 **as** July 8, 1996.

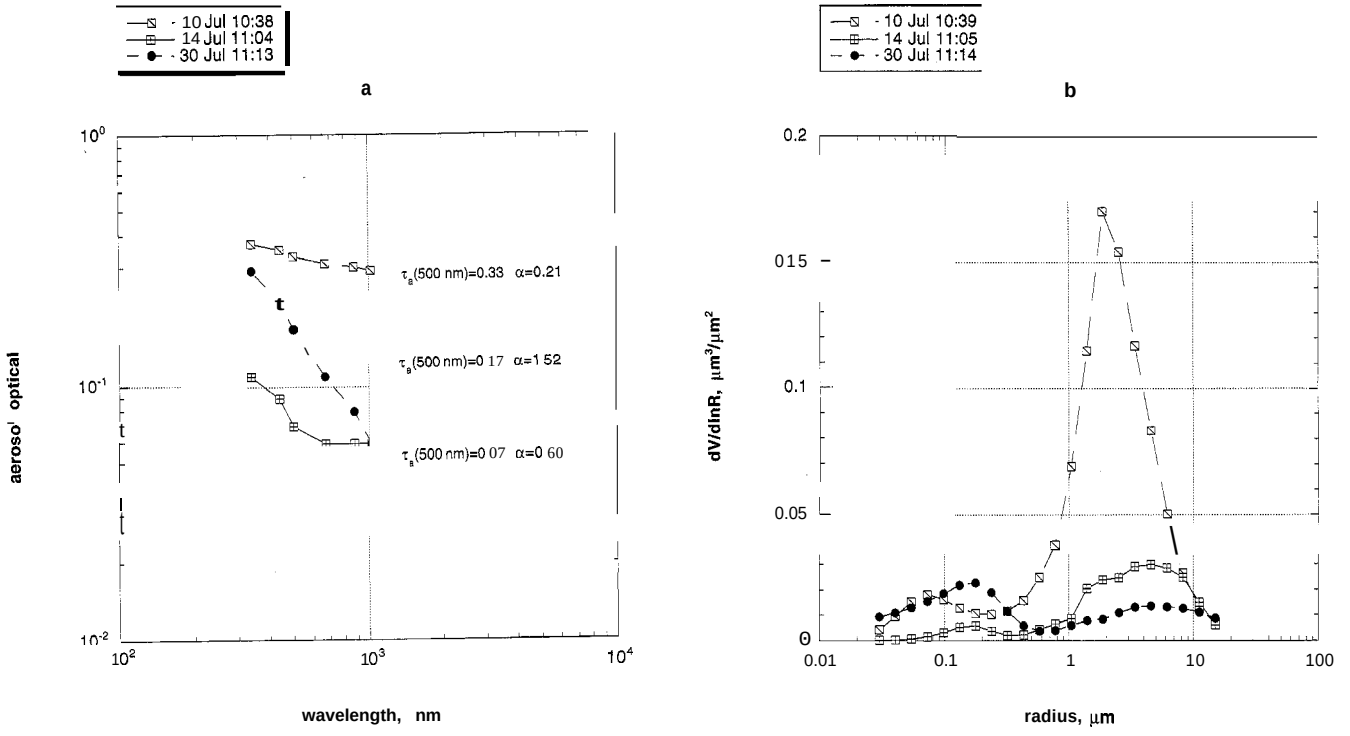

Figure 8. Aerosol optical depth spectra (a) and retrieved aerosol volume size distributions (b) for various aerosol sources for the Bermuda site.

conditions can be regarded as a mixture of the Atlantic and North American air.

The retrieved aerosol volume size distributions for various optical conditions are consistent with the aerosol optical depth spectral dependence (Figures 10a and 10b). The formal inversion of Figure 10b quantifies in detail the microstructure which one could infer in a first-order sense from the magnitude and spectral slope of the curves in Figure 10a. One can note a significant increase in the volume of coarse mode particles and corresponding decrease in the Angstrom parameter a for the Saharan dust event of July 12. The aerosol volume size distribution on July 8 showed a dominance of the fine aerosol fraction with a maximum at about 0.15 μm. The July **9** measurement of Figure 10 which was acquired in the vicinity of Bermuda, yielded smaller values of both optical depth and a. This latter behavior could be associated with an increasing influence of coarse mode maritime particles. The volume size distribution retrieval made for the July ***25*** data is in reasonable qualitative agreement with the other retrievals (Figure 10b) and optical depth measurements shown on Figure 10a.

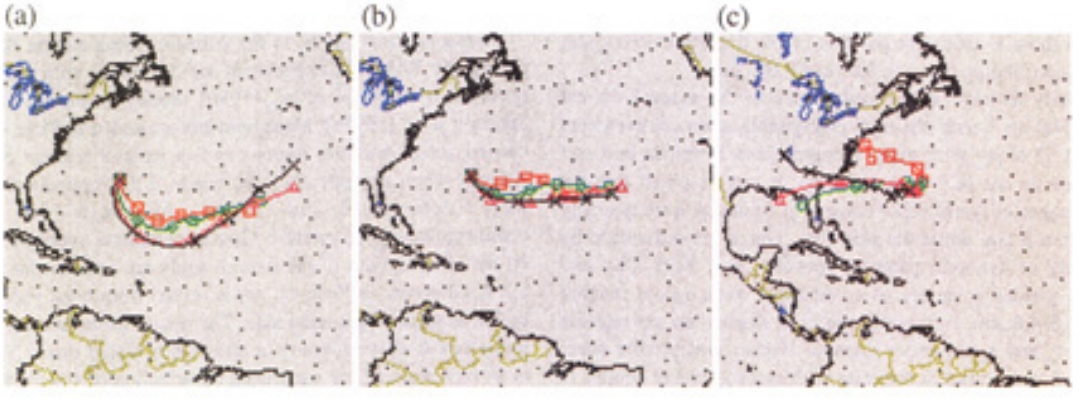

Plate 2. Selected set of 5-day back trajectories showing sources for air at 1000 mbar (red), **925** mbar (green), 850 mbar (purple), and 700 mbar (black) for the Bermuda site on July 10, 1200 UT (a), July **14, 1200 UT** (b), July **30,** 1200 UT (c).

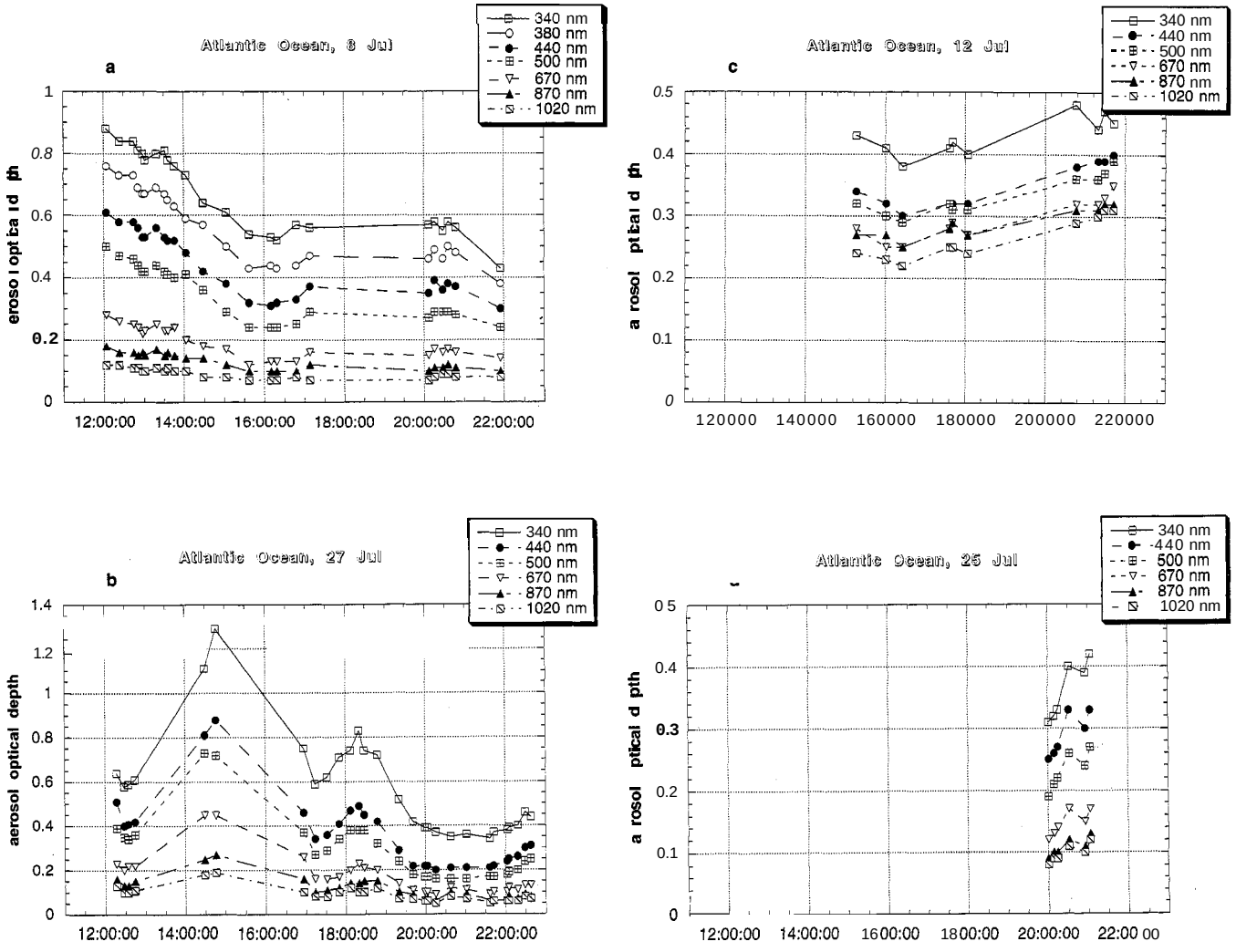

Figure 9. Diurnal variability of aerosol optical depth in the Atlantic Ocean on July **8** (a), July 27 (b), July 12 (c), and July 25 (d).

The dynamics of the volume size distribution and corresponding changes in aerosol optical depth and its spectral dependence on July 27 are demonstrated in Figure 11. The retrievals show a consistent position of the fine mode maximum at –0.08 ym (ranging between 0.07 and 0.095 ym).

The daily average ship-based values of the aerosol optical depth at 500 nm versus the total precipitable water are presented in Figure 12 along with daily averages from Bermuda and east coast sites for all July measurements. It can be noted that the daily averages of water vapor content in Bermuda were typically greater than 3 cm, while the ship data, which are influenced by the variety of synoptic patterns between New **York** City and Bermuda yielded a variety of precipitable water values ranging within 1.5-4.8 cm . Overall, there is almost no correlation between τ_a and water vapor content. Higher precipitable water amounts may not always correlate with aerosol optical depths; in continental east coast conditions, humid and polluted air are well correlated (Figure 3), but in a maritime environment despite high water vapor abundance, τ_a can be relatively small. Attempts to establish a correlation between aerosol optical depth and water vapor content may or may not be successful depending on the portion of continental and maritime $\tau_a(\lambda)$ in the data set.

Aerosol optical depths in the Atlantic Ocean and on Bermuda during the TARFOX experiment are consistent with the results reported by *Hoppel et al.* [1990], ***Reddy et al.*** [1990], and *Smirnov* ***et al.*** [1995b]. Measurements presented in Plate 4a were carried out in different regions and in various seasons over the Atlantic when synoptic analysis indicated that optical conditions were determined by North American air or a continental/maritime mixture. Optical parameter averages (τ_a and ***a)*** for specific days of the current study are listed in the botton. left-hand corner in Plate 4a, while results from cited papers may be found on the right-hand side. The scatter of the aerosol optical properties is evident, but α in all cases *is* higher than 1.1, which is an indication of the significant contribution of fine particles in the attenuation in the total atmospheric column. Plate 4b presents average aerosol optical depth spectral dependencies for Saharan dust episodes and remote (truly maritime) Atlantic air. As in

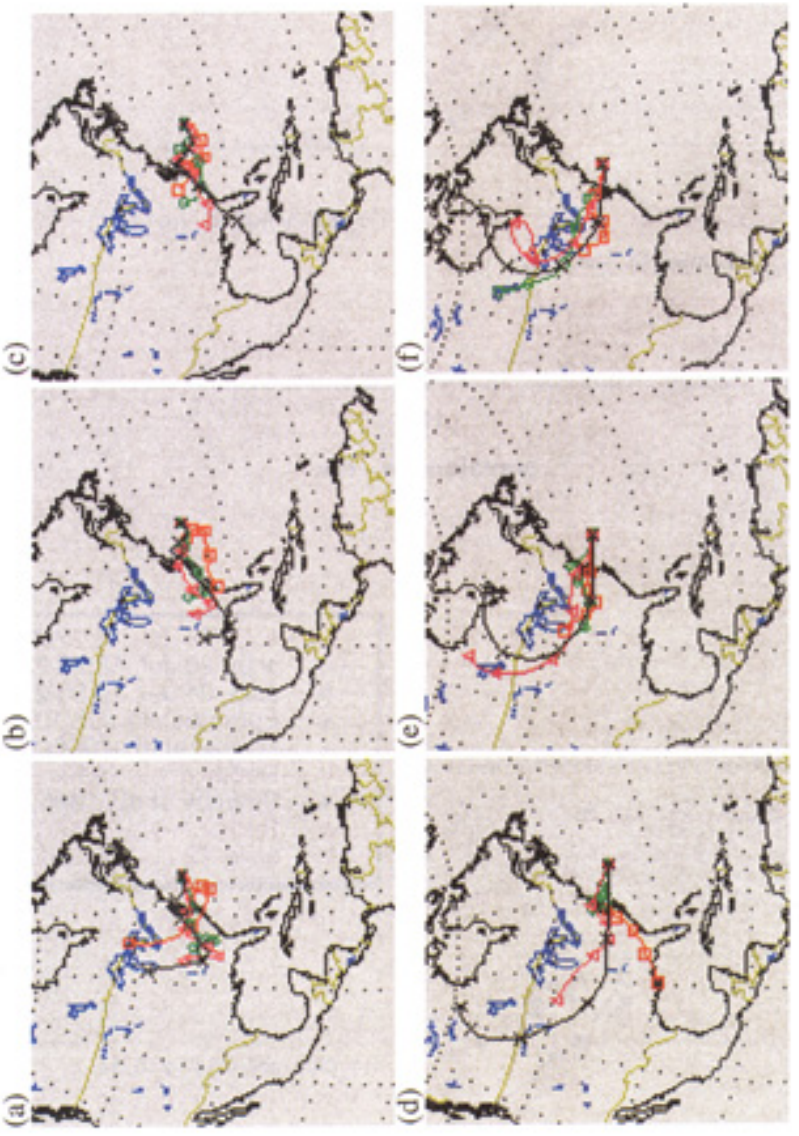

Plate 3. Selected set of 5-day back trajectories showing sources for air at 1000 mbar (red), 925 mbar (green), 850 mbar (purple), and 700 mbar (black) in the Atlantic Ocean on July 8, 1200 UT (a), 1800 UT (b), July 9, 0000 UT (c), July 27, 1200 UT (d), 1800 UT (e), July 28, 0000 UT (f).

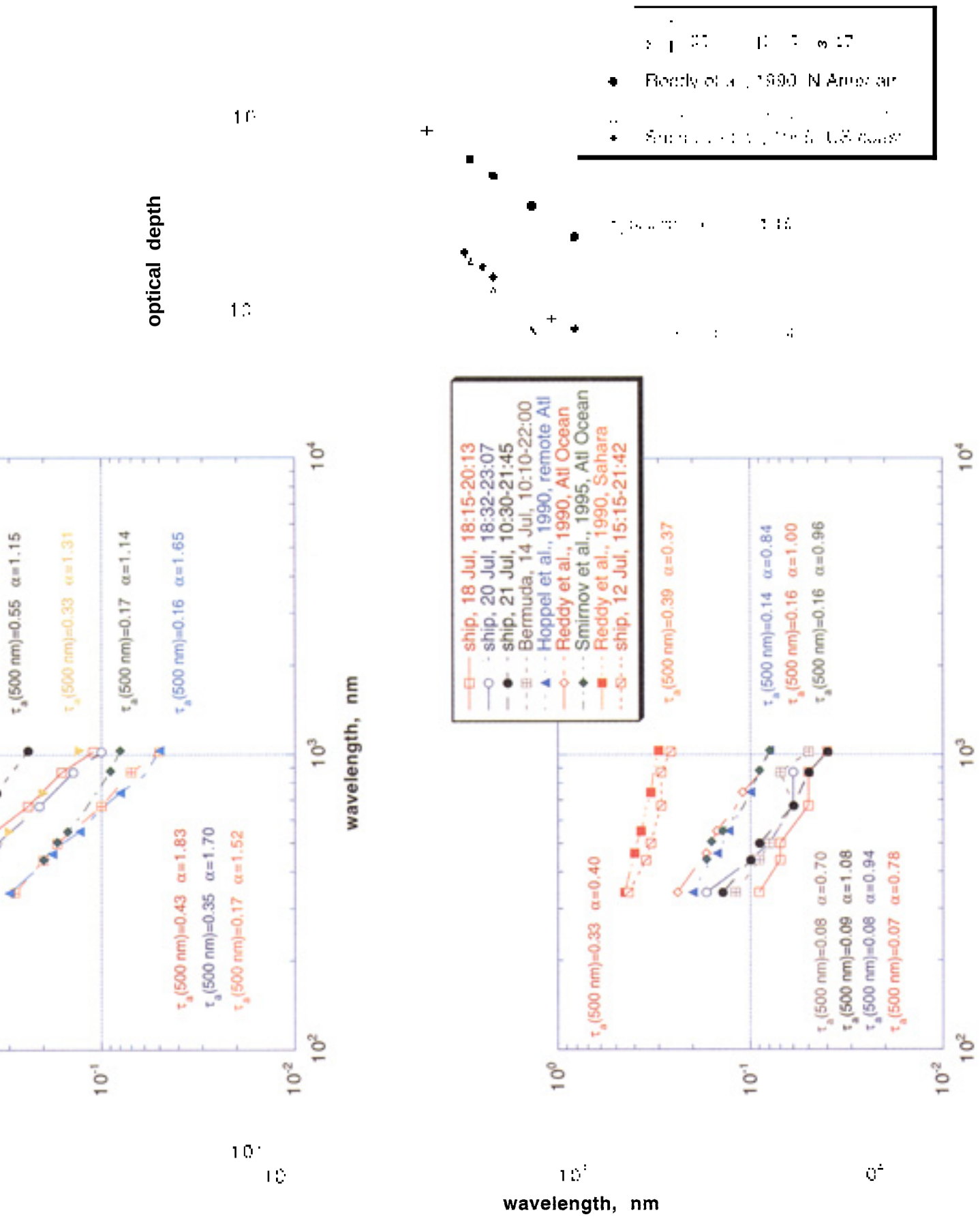

Plate 4. Aerosol optical depth spectra in various air masses above Atlantic Ocean.

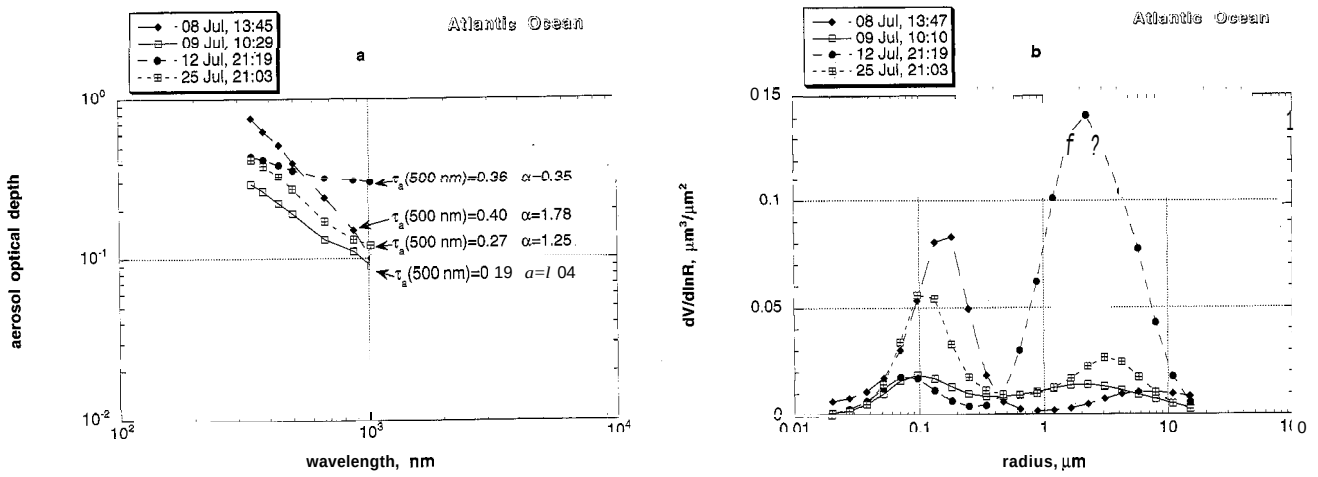

Figure 10. Aerosol optical depth spectra (a) and retrieved aerosol volume size distributions (b) for various aerosol sources in the Atlantic Ocean.

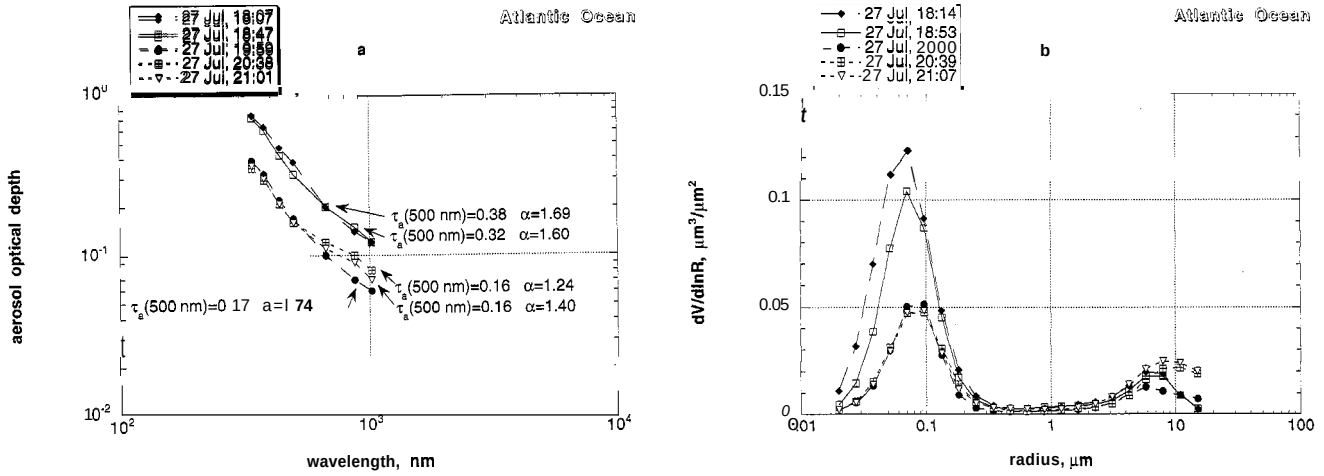

Figure 11. Aerosol optical depth spectra (a) and retrieved aerosol volume size distributions (b) in the Atlantic Ocean on July **27.**

Plate 4a, the optical parameters associated with the current study are listed in the left-hand comer, while cited data are on the right. Optical properties of the Saharan dust on July 12 are similar to the weak dust episode results reported by ***Reddy et al.*** [1990]. Remote Atlantic (or pure maritime) air occurred only on July 18 and yielded τ_a (500 nm) values, which were a factor of ***2*** smaller than reported results from other studies. The low optical depth and low Angstrom coefficient ***(a-0.7)*** for Atlantic air over Bermuda are consistent with a hypothesis of an enhanced input of coarse particles in the size distribution. Back trajectories showed that on July 20 and **21** the air in the measurement area was arriving from western and northern sectors of the North American continent, The continental influence can explain the slightly higher values of the Ängström parameter (a ~ 1) which one would have expected in a clean maritime environment [***Hoppel et al.,*** 1990; ***Smirnov et al.***, 1995a; ***Coroch*** *and Littfin*, 19981.

6. Conclusions

The principal conclusions drawn from our work can be summarized as follows:

1. Optical depths, Angstrom parameter values, aerosol volume size distributions measured or derived on various coastal sites, ships, and Bermuda during TARFOX generated a rather unique cross section of distinct atmospheric optical properties for different air masses and aerosol sources. In several cases the aerosol optical parameters at coastal sites were demonstrated to be spatially uniform within the same air masses (dimension ~1000 km).

2. Water vapor content in the total atmospheric column can be considered as an important characteristic of the air mass itself rather than the parameter responsible for the growth of atmospheric turbidity. Higher precipitable water amounts may not always correlate with the aerosol optical depth.

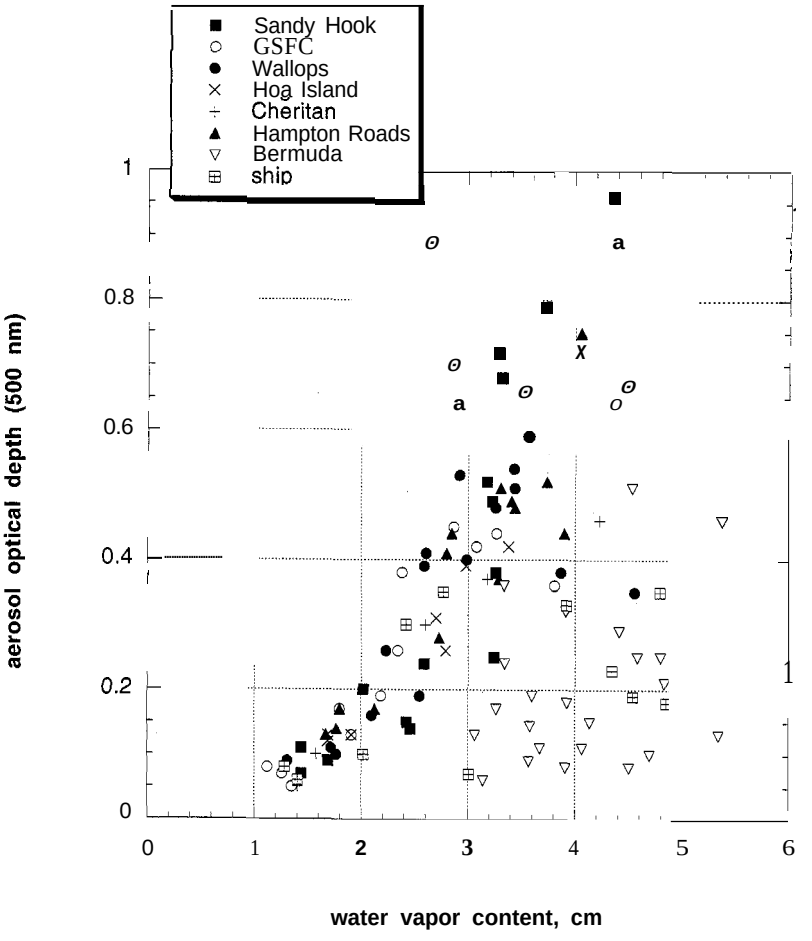

Figure 12. Scattergram of daily averages of aerosol optical depth at 500 nm versus water vapor content in centimeters of precipitable water.

Acknowledgments. The authors thank Robert Curran of NASA Headquarters and Michael King of the EOS Project Science Office for their support. The authors would like to thank Y.Kaufman and D.Tanre for fruitful discussions of certain issues.

References

Dubovik, O., B.N.Holben, M.D.King, A.Smirnov, T.F.Eck, S.Kinne, and I.Slutsker, A flexible inversion algorithm for retrieval of aerosol optical properties from Sun and sky radiance measurements, *Proc. ALPS'99, WK1-P-12*, 1-5, 1999a.

Dubovik, O., A.Smirnov, B.N.Holben, M.D.King, Y.J.Kaufman, T.F.Eck, and I.Slutsker, Accuracy assessments of aerosol optical properties retrieved from AERONET sun and sky radiance measurements, *J.Geophys.Res.*, in press, 1999b.

Eck, T.F., B.N.Holben, J.S.Reid, O.Dubovik, A.Smirnov, N.T.O'Neill, I.Slutsker, and S.Kinne, Wavelength dependence of the optical depth of biomass burning, urban, and desert dust aerosols, *J.Geophys.Res.*, in press, 1999.

Gerber, H., Probability distribution of aerosol backscatter in the lower marine atmosphere at CO_2 wavelengths, *J.Geophys.Res.*, 96, 5307-5314, 1991.

Goroch, A., and K.Littfin, Analysis of nephelometer observations during EOPACE IOP-7, ***Proceedings of the AGARD Conference on Environmental Effects on EO propagation,*** Naples, Italy, April 1998.

Halthore, R.N., T.F.Eck, B.N.Holben, and B.L.Markham, Sun photometric measurements of atmospheric water vapor column abundance in the 940-nm band, ***J.Geophys.Res., 102,*** 4343-4352, 1997.

Holben, B.N., et al., AERONET-A federated instrument network and data archive for aerosol characterization, ***Remote Sens.Environ.,*** *66*(1), 1-16, 1998.

Hoppel. W.A.. J.W.Fitzgerald, G.M.Frick, R.E.Larson, and E.J.Mack, Aerosol size distributions and optical properties found in the marine boundary layer over the Atlantic Ocean, *J.Geophys.Res.*, 95, 3659-3686, 1990.

Kaufman, **Y.J.,** D.Tanre, H.R.Gordon, T.Nakajima, J.Lenoble, R.Frouin, H.Grassl, B.M.Herman, M.D.King, and P.M.Teillet, Passive remote sensing of tropospheric aerosol and atmospheric correction for the aerosol effect, ***J.Geophys.Res., 102,*** 16,815-16,830, 1997.

Kotchenruther, R.A., P.V.Hobbs, and D.A.Hegg, Humidification factors for atmospheric aerosols off the mid-Atlantic coast of the United States, *J.Geophys.Res.*, 104,2239-2251, 1999.

Leaitch, W.R., et al., Physical and chemical observations in marine stratus during the 1993 North Atlantic Regional Experiment: Factors controlling cloud droplet number concentrations, ***J.Geophys.Res., 101***, 29,123-29.135, 1996.

Porter, J.N., and A.D.Clarke, Aerosol size distribution models based on in situ measurements, ***J.Geophys.Res.,*** 102,6035-6045, 1997.

Prospero, J.M., and T.N.Carlson, Vertical and areal distribution of Saharan dust over the western equatorial North Atlantic Ocean, *J.Geophys.Res., 77*, 5255-5265, 1972.

Quinn, P.K., V.N.Kapustin, T.S.Bates, and D.S.Covert, Chemical and

optical properties of marine boundary layer aerosol particles of the mid-Pacific in relation to sources and meteorological transport, *J.Geophys.Res.*, 101,6931-6951, 1996.

Reddy, P.J., F.W.Kreiner, J.J.DeLuisi, and Y.Kim, Aerosol optical depths over the Atlantic derived from shipboard Sun photometer observations during the 1988 Global Change Expedition, *Global Biogeochemical Cycles*, 4,225-240, 1990.

Remer, L.A., and Y.J.Kaufman, Dynamic aerosol model: Urban/industrial aerosol, *J.Geophys.Res.*, 103, 13,859-13,871, 1998.

Remer, L.A., Y.J.Kaufman, and B.N.Holben, Interannual variation of ambient aerosol characteristics on the east coast of the United States, *J.Geophys.Res.*, 104,2223-2231, 1999.

Russell, P.B., P.V.Hobbs, and L.L.Stowe, Aerosol properties and radiative effects in the United States East Coast haze plume: An overview of the Tropospheric Aerosol Radiative Forcing Observational Experiment (TARFOX), *J.Geophys.Res.*, 104, 2213-2222, 1999.

Sassen, K., M.K.Griffin, and G.Dodd, Optical scattering and microphysical properties of sub-visual clouds, and climatic implications, *J.Appl.Meteorol.*, 28.9 1-98, 1989.

Schmid, B., J.Michalsky, R.Halthore, M.Beauharnois, L.Harrison, J.Livingston, P.B.Russell, B.N.Holben, T.F.Eck, and A.Smirnov, Comparison of aerosol optical depth from four solar radiometers during the fall 1997 ARM Intensive Observation Period, *Geophys.Res.Lett.*, 26, 2725-2728, 1999.

Shettle, E.P., and R.W.Fenn, Models for the aerosols of the lower atmosphere and the effects of humidity variations on their optical properties, *Environ. Res. Pup.*, 676, 1-100, 1979.

Smirnov, A., Y.Villevalde, N.T.O'Neill, A.Royer, and A.Tarussov, Aerosol optical depth over the oceans: Analysis in terms of synoptic air mass types, *J.Geophys.Res.*, 100,16,639-16,650, 1995a.

Smirnov, A., O.Yershov, and Y.Villevalde, Aerosol optical depth in the Atlantic Ocean and Mediterranean Sea, *Proc. SPIE*, 2582, 203-214, 1995b.

O.Dubovik, T.F.Eck, B.N.Holben, N.T.O'Neill, I.Slutsker, and A.Smirnov, NASA Goddard Space Flight Center, Biospheric Sciences Branch, Code 923, Greenbelt, MD 20771. (asmirnov@spamer.gsfc.nasa.gov)

L.A.Remer, NASA Goddard Space Flight Center. Climate and Radiation Branch, Code 913, Greenbelt, MD 20771.

D.Savoie, Division of Marine and Atmospheric Chemistry, University of Miami, Miami, FL 32601.

(Received May 12, 1999; revised August 11, 1999;
accepted August 25, 1999.)